



INTERNATIONAL ATOMIC ENERGY AGENCY  
UNITED NATIONS EDUCATIONAL, SCIENTIFIC AND CULTURAL ORGANIZATION  
**INTERNATIONAL CENTRE FOR THEORETICAL PHYSICS**  
I.C.T.P., P.O. BOX 586, 34100 TRIESTE, ITALY, CABLE: CENTRATOM TRIESTE



H4.SMR/782-23

**Second Workshop on  
Three-Dimensional Modelling of Seismic Waves  
Generation, Propagation and their Inversion**

**7 - 18 November 1994**

***From Synthetic Seismograms  
to Seismic Hazard Assessment***

**F. Vaccari**

**Istituto di Geodesia e Geofisica  
Università di Trieste  
Trieste, Italy**

# Zoning of the Italian territory in terms of expected peak ground acceleration derived from complete synthetic seismograms

Giovanni Costa<sup>a</sup>, Giuliano Francesco Panza<sup>a,c</sup>, Peter Suhadolc<sup>a</sup> and Franco Vaccari<sup>a,b,1</sup>

<sup>a</sup>*Istituto di Geodesia e Geofisica, Università degli Studi di Trieste, Via dell'Università 7 34100 Trieste, Italy*

<sup>b</sup>*CNR, Gruppo Nazionale per la Difesa dai Terremoti, Roma, Italy*

<sup>c</sup>*International Center for Theoretical Physics, Strada Costiera 11, 34100 Trieste, Italy*

(Accepted after revision September 30, 1992)

## ABSTRACT

Costa, G., Panza, G.F., Suhadolc, P. and Vaccari, F., 1993. Zoning of the Italian territory in terms of expected peak ground acceleration derived from complete synthetic seismograms. In: R. Cassinis, K. Helbig and G.F. Panza (Editors), *Geophysical Exploration in Areas of Complex Geology, II*. *J. Appl. Geophys.*, 30: 149-160.

An automatic procedure for the seismic zonation of a territory is presented. The results consist of deterministic computation of acceleration time series distributed on a regular grid over the territory. For the estimation of the accelerations, complete synthetic seismograms are computed by the modal summation technique. A first rough zonation can be accomplished by considering a map showing the distribution of peak ground acceleration. In this work the new procedure has been applied to the Italian territory. The structural and source models necessary to compute the synthetic signals have been fixed after an extensive bibliographic research. Seismogenic areas have been defined in the framework of the GNDT (Gruppo Nazionale per la Difesa dai Terremoti of the Consiglio Nazionale delle Ricerche, Rome) research activities dedicated to the definition of the kinematic model of Italy. Information on historical and recent seismicity has been taken from the most updated Italian earthquake catalogues. The estimated peak ground accelerations have been found to be compatible with available data, both in terms of intensity (historical earthquakes) and accelerations (recent earthquakes).

## Introduction

The zonation of a territory in terms of seismic hazard is an essential preventive countermeasure in countries with high seismic risk, especially for densely populated areas. Maximum expected peak ground acceleration (PGA), at different frequencies, is a very important parameter considered by civil engineers when designing or reinforcing constructions.

We have developed a deterministic procedure which allows us to estimate PGA (routinely at frequencies as high as 10 Hz) starting from the available information on Earth struc-

ture parameters, seismic sources, and the level of seismicity of the investigated area. Theoretical accelerations are computed by the modal summation technique (Panza, 1985; Florsch et al., 1991). The use of synthetic seismograms allows us to estimate, in a realistic way, the seismic hazard, also in those areas for which scarce (or none) historical or instrumental information is available. It is also possible to simulate quite easily different kinds of source mechanisms, to consider different structural models, and to compare the relative results in order to evaluate the influence of each parameter. To reduce the amount of computations, the seismic sources have been grouped in homogeneous seismogenic areas, and for each group the representative focal mechanism has

<sup>1</sup>Authors listed in alphabetical order.

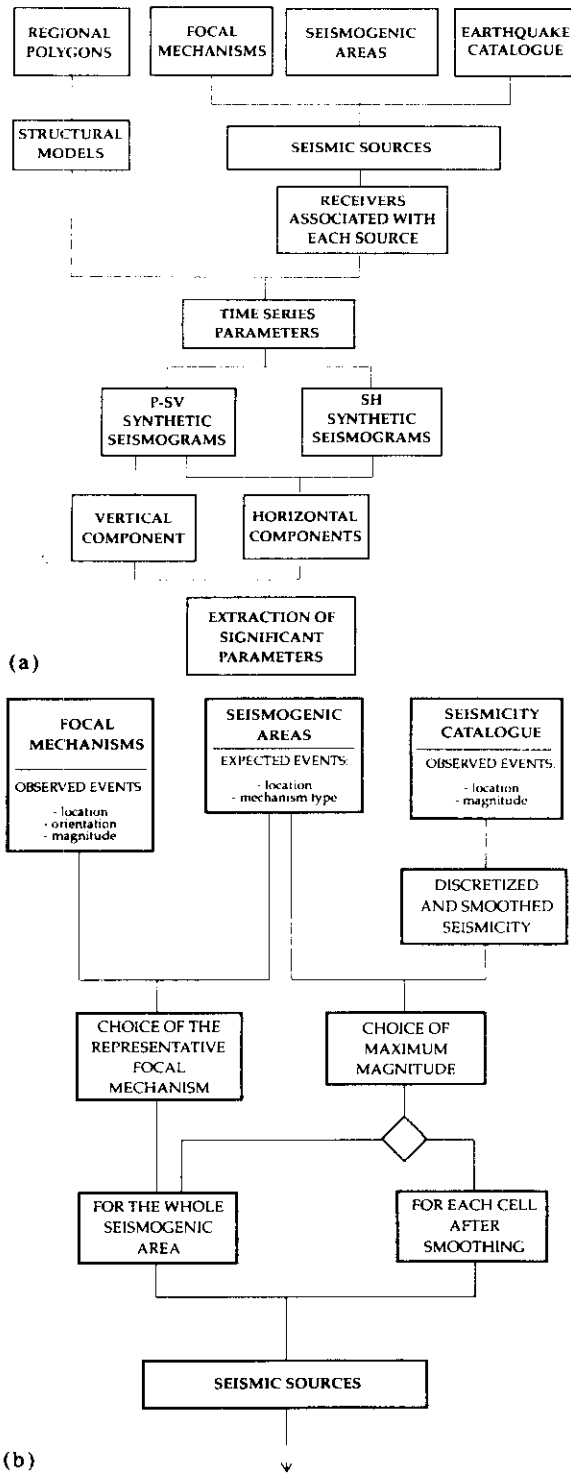


Fig. 1. (a) Flow-chart of the procedure. (b) Detail concerning the definition of seismic sources.

been kept constant. The seismic moment associated with each source is determined from the analysis of the maximum magnitude observed in the epicentral area in the past.

One way of representing the result of the procedure is to analyse the synthetic seismograms and to map the distribution of PGA over the investigated territory. The synthetic signals used for the prediction of the accelerations can be conveniently used as input data for more detailed zoning, based on the 2-D modelling of wave propagation (Fäh et al., 1990; Iodice et al., 1992). In this way, also the local soil effects can be taken into account.

The flow-chart of the procedure is shown in Fig. 1. In the following text, references to the flow chart are written in *italics*.

## Data

To compute the synthetic seismograms, the structures containing the source and the receivers must be defined, as well as the source characteristics. On the basis of the geologic characteristics, the Italian territory has been divided into 16 *polygons* (Fig. 2). Then a flat, layered *structural model* has been associated with each polygon. The different layers are described by their thickness, density, P- and S-wave velocities, and attenuation. The layering has been defined after an extensive bibliographic research, taking into account available DSS data (e.g. Schütte, 1978; Italian Explosion Seismology Group and Institute of Geophysics ETH, 1981; Nicolich, 1981; Bottari et al., 1982; Miller et al., 1982; Kern and Schenk, 1985; Scarascia and Pellis, 1985; Nicolich, 1989; Nicolas et al., 1990) and indirectly relevant data (e.g. Woollard, 1975).

The definition of the *seismic sources* has required the analysis of several data sets. To limit the spatial distribution of sources, we have used the 57 *seismogenic areas* (see Fig. 3) defined by the GNDT (1992) on the basis of seismological data and seismotectonic observations (e.g. Patacca et al., 1993).

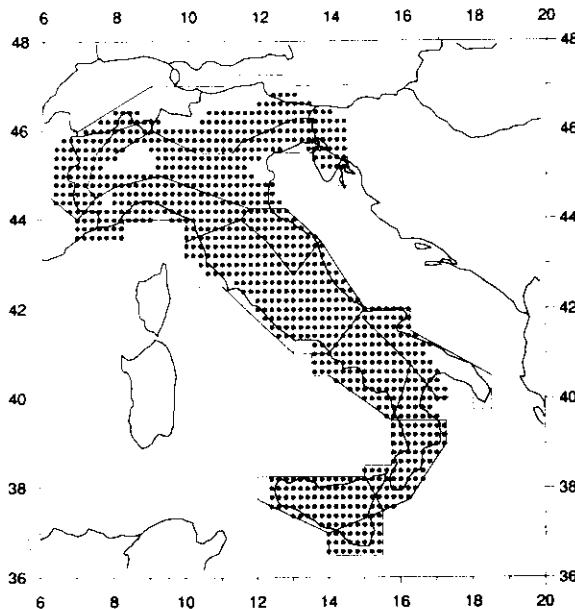


Fig. 2. Regional polygons associated with different structural models. The grid of dots represent the location of the receivers where synthetic seismograms have been computed.

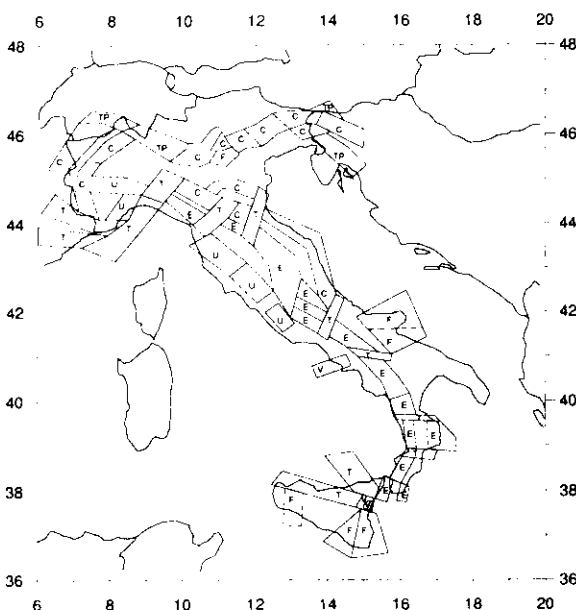


Fig. 3. Seismogenic zones defined by GNDT (1992). C=compressional areas; E=extensional areas; F=areas of fracture in foreland zones; T=transition areas; TP=areas of transpression; U=uncertain areas; V=volcanic areas.

For the definition of the source mechanisms, 305 fault-plane solutions, distributed over the whole territory, have been grouped in a database (Suhadolc, 1990; Suhadolc et al., 1992). The computer file contains a standard definition of the *focal mechanisms*, both as a function of strike, dip and rake of the nodal planes and as a function of the direction of compressional, tensional and null axes.

For the analysis of seismicity, an *earthquake catalogue* (PFGING) has been prepared, merging the data from the PFG (1985) catalogue, for the period 1000–1979, with the data from ING (1980–1991) bulletins, for the period 1980–1991. The original catalogues have been corrected for some obvious mistakes, like the presence of double or multiple events, time disorder and evident errors in the focal depths. Furthermore, only main shocks shallower than 50 km have been considered, removing aftershocks according to the algorithm suggested by Keilis-Borok et al. (1980).

We have considered only earthquakes that occurred within the PFG polygon (PFG, 1985). Therefore, the seismicity might be underestimated near political borders, and this could also have influenced the results (PGA distribution) in the regions close to these boundaries.

### Computations

To derive the distribution of the maximum observed magnitude over the territory, the image of the seismicity given by the earthquake catalogue has been smoothed. At first, the area has been subdivided into  $0.2^\circ \times 0.2^\circ$  cells. Each cell has been assigned the magnitude value of the most energetic event that occurred within it. The smoothing obtained through this discretization, however, was not found to be satisfactory, because not each cell does contain a statistically meaningful number of events. Therefore, the maximum magnitude to be associated with each cell has been searched for also in the cell surroundings, through the ap-

plication of a centred smoothing window. More details about the discretization and smoothing of seismicity are given in Appendix 1.

For the definition of the seismic sources that are used to generate the synthetic seismograms, only the cells located within a seismogenic area are retained. The map shown in Fig. 4 is the result of the application of this method to the PFGING earthquake catalogue.

A double-couple point source is then placed

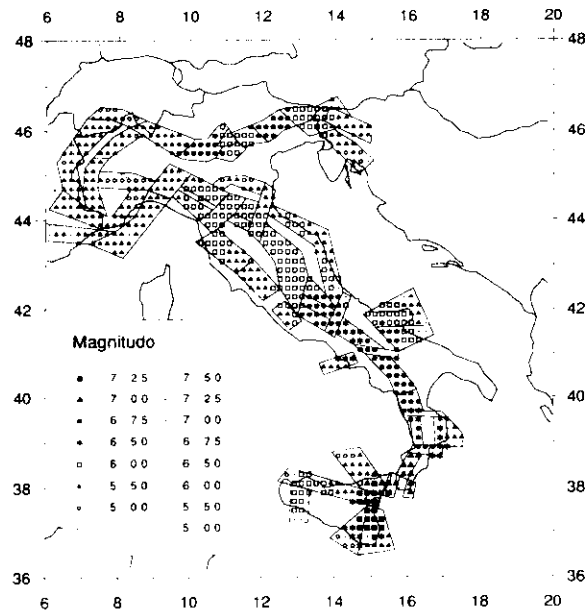


Fig. 4. Smoothed magnitude distribution for the cells belonging to the seismogenic zones shown in Fig. 3.

TABLE I

The moment-magnitude relation

Magnitude	$M_{0(1\text{Hz})}$ (N·m)
$8.00 \geq M > 7.75$	$4.00 \times 10^{18}$
$7.75 \geq M > 7.50$	$2.50 \times 10^{18}$
$7.50 \geq M > 7.25$	$1.60 \times 10^{18}$
$7.25 \geq M > 7.00$	$1.25 \times 10^{18}$
$7.00 \geq M > 6.75$	$5.00 \times 10^{17}$
$6.75 \geq M > 6.50$	$3.15 \times 10^{17}$
$6.50 \geq M > 6.00$	$1.60 \times 10^{17}$
$6.00 \geq M > 5.50$	$4.00 \times 10^{16}$
$5.50 \geq M > 5.00$	$1.40 \times 10^{16}$
$5.00 \geq M$	$4.00 \times 10^{15}$

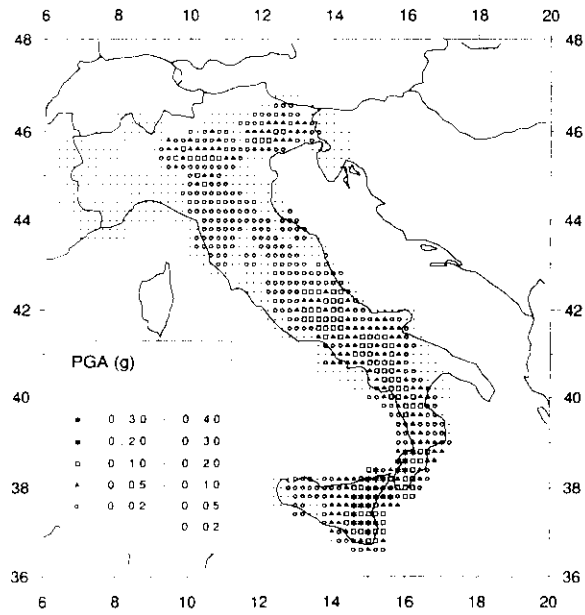


Fig. 5. Estimated distribution of horizontal peak ground acceleration.

TABLE 2

The intensity-acceleration relation

Intensity	Acceleration <sup>1</sup>	
	$\text{cm} \cdot \text{s}^{-2}$	$g$
XII	492.5	0.50
XI	370.9	0.38
X	284.4	0.29
IX	222.1	0.23
VIII	176.5	0.18
VII	142.9	0.15
VI	117.7	0.12
V	98.7	0.10
IV	84.3	0.09

<sup>1</sup>Estimates from Boschi et al., 1969.

in the centre of each cell. The orientation of the double couple associated with each source is obtained from the database of the fault-plane solutions. For each seismogenic area, a representative focal mechanism is selected through an automatic procedure. As a first simple hypothesis, the tensor elements of these mechanisms have been defined as the arithmetic average of the tensor elements of the available

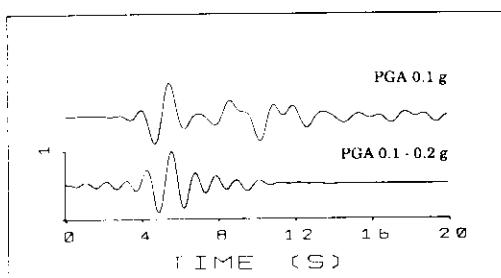


Fig. 6. Comparison between NS acceleration recorded at the station of Sturno during the Irpinia earthquake of 23 November 1980 (above) and one synthetic signal computed for that area (below) on the basis of the procedure described in this work. Accelerations have been low-pass filtered with a cut-off frequency of 1 Hz.

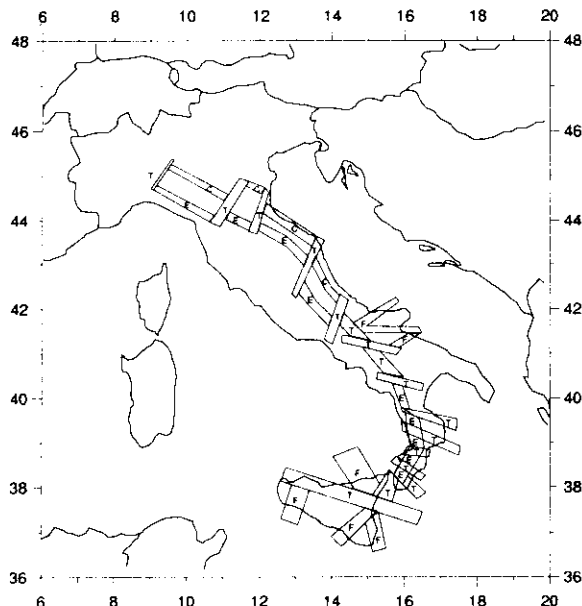


Fig. 7. Seismogenic zones given by GNDT as a preliminary result in the seismogenic zonation of the Italian territory. This model, that we refer to as Model A, must be compared with the one shown in Fig. 3. C=compressional areas; E=extensional areas; F=areas of fracture in fore-land zones; T=transition areas.

mechanisms. This procedure appears to be reasonable when the mechanisms are not too different to average, and this condition has been checked for each seismogenic area.

Once the structures and the sources have been defined, *receivers* are placed on a grid

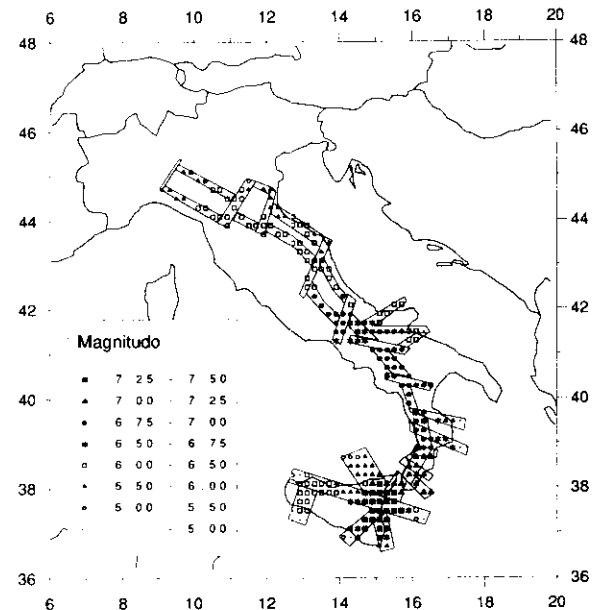


Fig. 8. Smoothed magnitude distribution for the cells belonging to the seismogenic zones shown in Fig. 7.

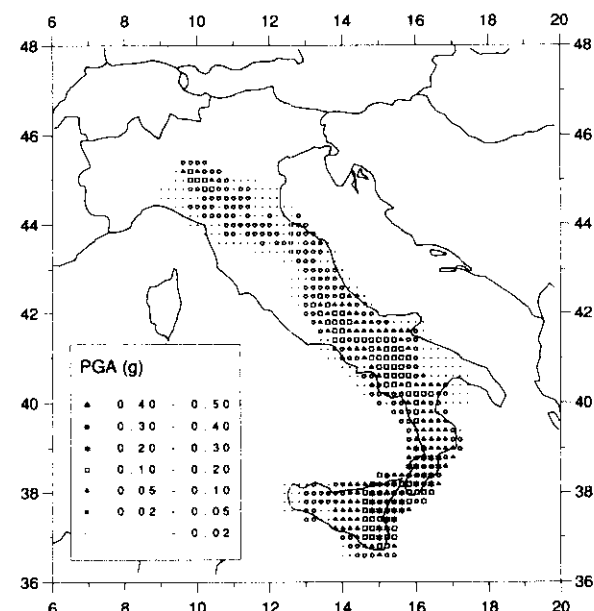


Fig. 9. Estimated distribution of the horizontal peak ground acceleration obtained using the seismogenic zones of Fig. 7. For a stability test it should be compared with Fig. 5.

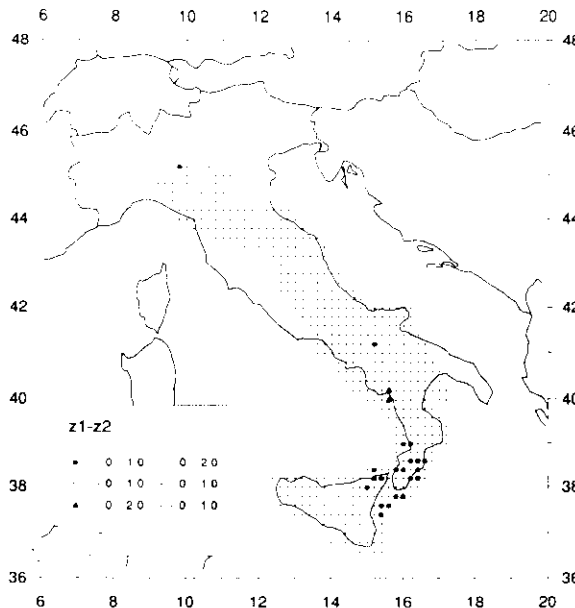


Fig. 10. Map of the relevant discrepancies between the PGA values shown in Figs. 5 and 9.

( $0.2^\circ \times 0.2^\circ$ ) covering the whole territory and synthetic seismograms are efficiently computed by the modal summation technique (Panza, 1985; Florsch et al., 1991). In this first example, the synthetic signals are computed for an upper frequency content of 1 Hz, and the point-source approximation is still acceptable. This is fully justified by practical considerations, because, for instance, several-story buildings have a peak response in the frequency range below 1 Hz (e.g. Manos and Demosthenous, 1992). When shorter periods are considered, it will be no longer possible to neglect the finite dimensions of the faults and the rupturing process at the source.

To reduce the number of the computed seismograms, the source-receiver distance is kept below an upper threshold, which is taken to be a function of the magnitude associated with the source. The maximum source-receiver distance has been set equal to 25, 50, and 90 km for  $M < 6$ ,  $6 \leq M < 7$  and  $M \geq 7$ , respectively. All seismograms have been computed for a constant hypocentral depth (10 km), but it is also possible to assign to each source an average

depth determined from the analysis of catalogues of past seismicity. The reason to keep the hypocentral depth fixed and shallow is to be found in the large errors affecting the hypocentral depth estimates in the PFGING catalogue and in the fact that strong ground motion is mainly controlled by shallow sources (e.g. Vaccari et al., 1990).

*P-SV* (radial and vertical components) and *SH* (transverse component) *synthetic seismograms* are originally computed for a seismic moment of  $1 \times 10^{-7}$  N·m. The amplitudes are then properly scaled according to the (smoothed) magnitude associated with the cell of the source. For the moment-magnitude relation, we have chosen the one given by Boore (1987). To obtain the values given in Table 1, which are valid for the frequency of 1 Hz, we have used the scaling law proposed by Gusev (1983). The idea of a constant magnitude within each seismogenic area (choosing the maximum available value) has been discarded because, for the larger seismogenic areas, it leads to an over-estimation of the seismicity.

At each receiver, the horizontal components are first rotated to a reference system common to the whole territory (N-S- and E-W-directions) and then the vector sum is computed. For the *significant parameters* representative of the strong ground motion we have, for the moment, focused our attention on the peak ground acceleration values (PGA). As we compute the complete time series, we are not limited to this choice, and it is also possible to consider other parameters, like Arias (1970) intensity or other integral quantities that can be of interest in seismic engineering. Because recordings of many different sources are associated to each receiver, but one single value is to be plotted on a map (Fig. 5), only the maximum value of the analysed parameter is considered.

## Discussion and conclusions

The intensity-acceleration relation proposed by Boschi et al. (1969) has been used to

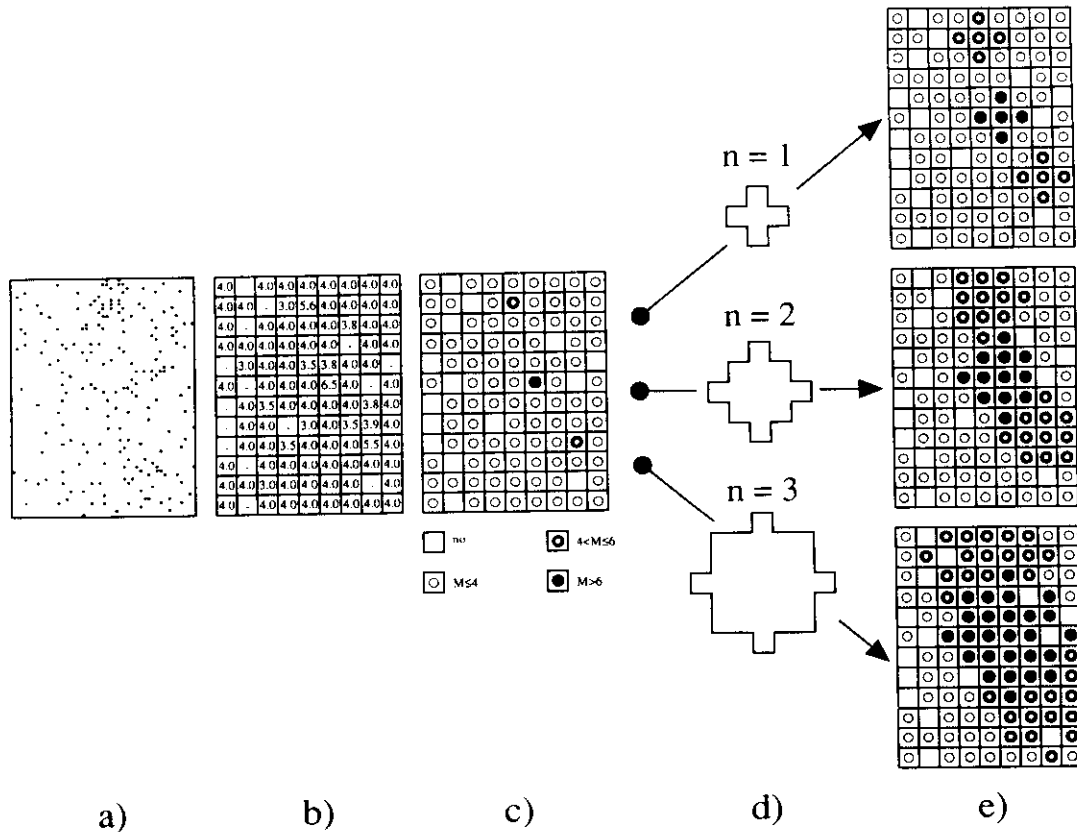


Fig. 11. Discretization and smoothing of seismicity. a=distribution of epicentres; b=definition of cells and choice of maximum magnitude; c=graphic representation of b; d=smoothing windows of radius  $n=1$ ,  $n=2$ ,  $n=3$ ; e=smoothed distribution of magnitude.

compare the results of Fig. 5 with the historical data, for which only macroseismic intensity estimates exist (see Table 2). We have checked that the computed PGA values are compatible with the above mentioned relation.

A more quantitative check has been made using the observed accelerograms recorded during the Irpinia earthquake on 23 November 1980. It is well known that the source rupturing process of that event is very complex (e.g. Bernard and Zollo, 1989), and the dimension of the source has been estimated to be of the order of several tens of kilometres. Nevertheless, it seems that the signal recorded at the station of Sturno is mostly due to a single sub-event that occurred rather close to the

station itself, while the energy contributions coming from other regions of the source seem irrelevant (Vaccari et al., 1990). We have low-pass filtered the NS accelerogram recorded at Sturno with a cut-off frequency at 1 Hz to compare it with one of the computed signals for the Irpinia region (Fig. 6). The early phases and the PGA of the two time series are in very good agreement. The late part of the observed recording is more complicated and this is related to the complexity of the source, which has been neglected in the computation of the synthetic signal.

The definition of seismogenic structures of the Italian territory, given by GNDT (1982), is the final result of a fruitful cooperation be-

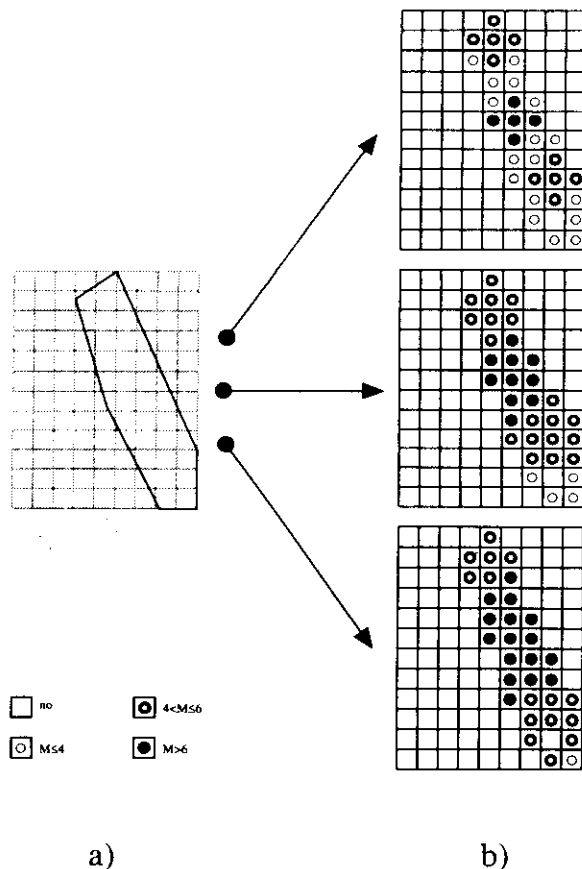


Fig. 12. Hypothetical seismogenic zone (a) and its intersection with the example data of Fig. 11e (b).

tween structural geologists and seismologists from all over Italy. In developing the project, several proposals have been made and some provisional hypothesis have been considered. Taking advantage of those existing alternatives, it has been possible to test the stability of our results, namely the PGA distribution, versus the distribution of seismogenic structures. Model *A* is one intermediate result of the GNDT project, as it does not include the Alpine Arc (Fig. 7) and can be compared with the more recent, presently accepted, model of Fig. 3, which was used to compute the PGA distribution shown in Fig. 5. In the common regions, some relevant differences can be evidenced in the Lazio and Toscana regions, as well as in the

Gargano peninsula. Furthermore, in the more recent model, the Calabrian Arc is characterised by a much more simplified zonation. The smoothed magnitudes associated with the seismogenic zones of Model *A* are given in Fig. 8. Figure 9 shows the PGA distribution obtained using Model *A* and should be compared with Fig. 5. It can be noticed that in the common areas the regions where maximum accelerations are expected to occur are almost the same, and also the PGA values do not differ too much. Relevant discrepancies, between 0.1 and 0.2 g, can only be found in relation with the Calabrian Arc (see Fig. 10) where, due to the larger spatial extension of seismogenic areas, Model *A* implies PGA values also in the class 0.40–0.50 g.

This comparison shows one important advantage of the procedure, namely the possibility of easily testing the influence of any parameter that is used as input data. An important stability test will be performed as soon as the revised earthquake catalogue by GNDT will be available. Stability tests are currently being performed analysing the catalogues in different periods of time.

#### Appendix 1. Discretization and smoothing of seismicity

The first problem to tackle in the definition of seismic sources is the handling of seismicity data. What is needed for the procedure described in this paper and will be used in the computation of synthetic seismograms is a distribution over the territory of the maximum magnitude. Data available from earthquake catalogues are, on the contrary, discrete and punctual. Furthermore, a 2-dimensional distribution requires a large amount of samples to be well determined, but earthquake catalogues are both incomplete and affected by errors, so a smoothed distribution is preferable (Panza et al., 1990). A smooth distribution can be misleading in the fact that it assigns some values also to areas where data are absent. To

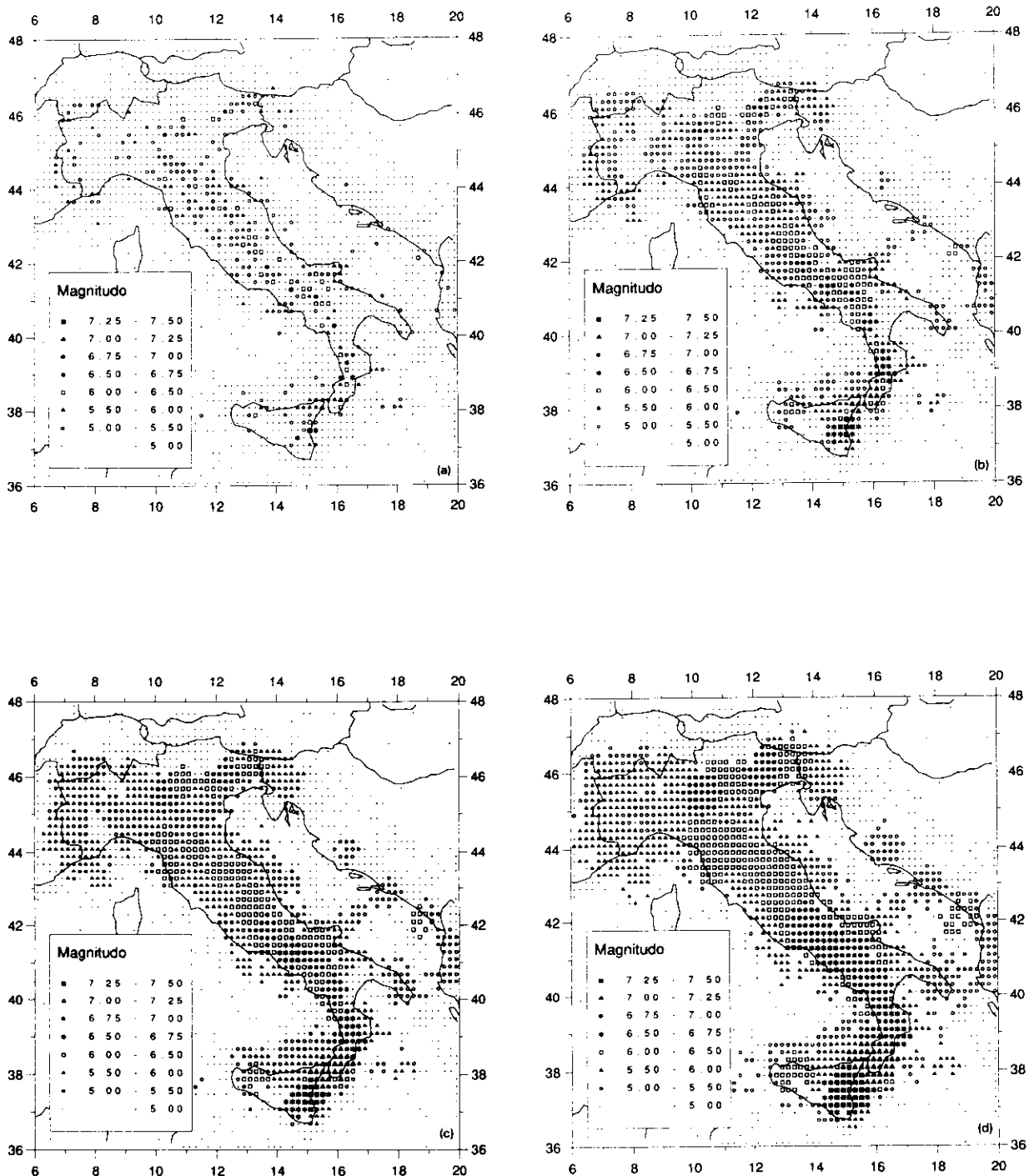


Fig. 13. Magnitude distribution after the application of discretization and smoothing to the seismicity data given in catalogue PFGING after aftershock removal. Radius of smoothing window: (a)  $n=0$ ; (b)  $n=1$ ; (c)  $n=2$ ; (d)  $n=3$ .

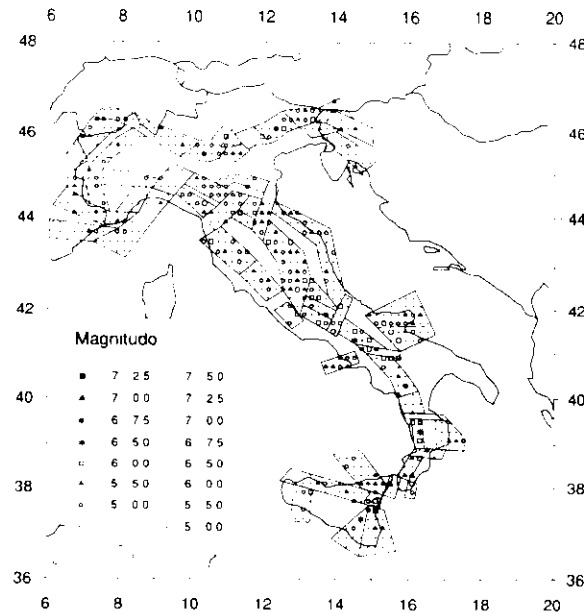


Fig. 14. Intersection between the seismogenic zones of Fig. 3 and the seismicity image of Fig. 13a.

avoid this drawback, we have decided to represent seismicity by cells. The size of the cells can be related with errors in the location of earthquakes. On the basis of experience (Suhadolc, 1990) the dimensions of  $0.2^\circ \times 0.2^\circ$  have been chosen, even if for historical earthquakes such a resolution could be considered optimistic.

The smoothing procedure is shown in Fig. 11. At first, the punctual distribution of epicentres given in Fig. 11a is discretised into cells (Fig. 11b) and the maximum magnitude of the events pertinent to each cell is retained. In case the earthquake catalogue contains different estimates of the magnitude (e.g. magnitude computed from body waves, from surface waves, from macroseismic intensity), the maximum between them is considered. It is then convenient to represent the data graphically, where symbols are associated with magnitude ranges (Fig. 11c).

In most cases, the smoothing obtained by just considering cells is not enough, because from a statistical point of view single cells do not con-

tain a meaningful number of events. A centered smoothing window is then considered. Earthquake magnitudes are analysed not only in the central cell, but also in neighboring ones. The maximum value of magnitude found in the window is assigned to the central cell only if the cell itself contains a minimum number of earthquakes. For this purpose, several thresholds have been tested (one to four earthquakes): the increase in the threshold is related to a more stable representation of seismicity, because sporadic events, that could be the result of mislocations or singularities of the seismic regime, are eliminated. We have noticed that only areas with very low seismicity, not included in the seismogenic areas shown in Fig. 3, are sensible to modifications of the threshold in the range 1 to 3. Therefore, taking into consideration only the seismogenic areas, stability is already ensured if the lower threshold (one earthquake) is selected.

Three possible smoothing windows are shown in Fig. 11d. Their "radius" is expressed in terms of number of cells,  $n$ . In the example, the values  $n=1$ ,  $n=2$  and  $n=3$  are considered. By applying those windows to the distribution of Fig. 11c, the results of Fig. 11e are obtained. At a first glance, it appears that the distribution of maximum magnitude given by the window with  $n=3$  is quite exaggerated with respect to the starting data of Fig. 11c, but its intersection with an hypothetical seismogenic area (shown in Fig. 12a) gives quite reasonable results (Fig. 12b).

The smoothing algorithm has been applied to the catalogue of main shocks for the Italian territory. Windows of radius  $n=0$  (which corresponds to considering just the central cell),  $n=1$ ,  $n=2$  and  $n=3$  have been used, obtaining the results shown in Fig. 13a-d, respectively. The intersection of the map of Fig. 13d with the seismogenic areas of Fig. 3, defined by GNDT (1992), is already shown in Fig. 4. The radius  $n=3$  has been selected because a good degree of homogeneity in the distribution of magnitude seems appropriate within each seis-

mogenic area. This condition is not verified if the smoothing is not applied (see Fig. 14).

### Acknowledgements

This study has been made possible by the CNR contracts 90.02382.CT15, 90.01026.PF54. We would like to thank ENEA for allowing us the use of the IBM3090E computer at the ENEA INFO BOL Computer Center. This research has been carried out in the framework of the activities of the ILP Task Group II.4.

### References

Arias, A., 1970. A measure of earthquake intensity. In: R. Hansen (Editor), *Seismic Design for Nuclear Power Plants*. Cambridge, MA, pp. 438-483.

Bernard, P. and Zollo, A., 1989. The Irpinia (Italy) 1980 earthquake: detailed analysis of a complex normal faulting. *J. Geophys. Res.*, 94: 1631-1647.

Boore, D.M., 1987. The prediction of strong ground motion. In: M.Ö. Erdik and M.N. Toksöz (Editors), *Strong Ground Motion Seismology*. Reidel, Dordrecht, pp. 109-141.

Boschi, E., Caputo, M. and Panza, G.F., 1969. Stability of seismic activity in Italy with special reference to Garfagnana, Mugello and Forlivese. *Rapp. CNEN RT/ING(69)24*, pp. 1-24.

Bottari, A., Caccamo, D., Carapezza, E., Cosentino, M., Cosentino, P., Federico, B., Fradella, P., Hoang Trong, P., Lo Giudice, E., Lombardo, G., Neri, G. and Patanè, G., 1982. Crustal regional travel times of P and S waves in Sicily. CNR, Roma. *Atti 2° Conv. GNGTS*, pp. 605-614.

Fäh, D., Suhadolc, P. and Panza, G.F., 1990. Estimation of strong ground motion in laterally heterogeneous media: modal summation-finite differences. *Proc. 9th Eur. Conf. Earthquake Eng.*, Sept. 11-16, 1990, Moscow. 4A, pp. 100-109.

Florsch, N., Fäh, D., Suhadolc, P. and Panza, G.F., 1991. Complete synthetic seismograms for high-frequency multimode Love waves. *Pure Appl. Geophys.*, 136: 529-560.

GNDT, 1992. Convegno Nazionale sul Modello Sismotettonico d'Italia. Milano, 25-26 May.

Gusev, A.A., 1983. Descriptive statistical model of earthquake source radiation and its application to an estimation of short period strong motion. *Geophys. J.R. Astron. Soc.*, 74: 787-800.

ING, 1980-1991. Istituto Nazionale di Geofisica. Seismological reports. ING, Roma.

Iodice, C., Fäh, D., Suhadolc, P. and Panza, G.F., 1992. Un metodo generale per la zonazione sismica rapida ed accurata di grandi metropoli: applicazione alla città di Roma. *Rend. Accad. Lincei*, 3: 195-217.

Italian Explosion Seismology Group and Institute of Geophysics, ETH, Zürich, 1981. Crust and upper mantle structures in the Southern Alps from deep seismic sounding profiles (1977, 1978) and surface waves dispersion analysis. *Boll. Geofis. Teor. Appl.*, 23: 297-330.

Keilis-Borok, V.I., Knopoff, L., Rotwain, I.M. and Sidorenko, T.M., 1980. Bursts of seismicity as long-term precursors of strong earthquakes. *J. Geophys. Res.*, 85: 803-812.

Kern, H. and Schenk, V., 1985. Elastic wave velocities from a lower crustal section in Southern Calabria (Italy). *Phys. Earth Planet. Inter.*, 40: 147-160.

Manos, G.C. and Demosthenous, M., 1992. Design of R.C. structures according to the Greek Seismic Code Provisions. *Bull. ISEE*, 26: 559-578.

Miller, H., Mueller, St. and Perrier, G., 1982. Structure and dynamics of the Alps: a geophysical inventory. In: H. Berkhemer and U. Hsü (Editors) *Alpine-Mediterranean Geodynamics*. Am. Geophys. Union, Geophys. Ser., 7, pp. 175-203.

Nicolas, A., Polino, R., Hirn, A., Nicolich, R. and ECORS-CROP Working Group, 1990. ECORS-CROP traverse and deep structures of the Western Alps: a synthesis. In: R. Roure, P. Heitzman and R. Polino (Editors), *Deep Structure of the Alps*. Mém. Soc. Geol. Fr. Ital. Suisse, pp. 15-27.

Nicolich, R., 1981. Il profilo Latina-Pescara e le registrazioni mediante OBS nel Mar Tirreno. CNR, Roma. *Atti 1° Conv. GNGTS*, pp. 621-634.

Nicolich, R., 1989. Crustal structures from seismic studies in the frame of the European Geotraverse (Southern Segment) and CROP projects. *Atti Conv. Lincei*, 80: 41-61.

Panza, G. F., 1985. Synthetic seismograms: The Rayleigh waves modal summation. *J. Geophys.*, 58: 125-145.

Panza, G. F., Prozorov, A. and Suhadolc, P., 1990. Is there a correlation between lithosphere structure and statistical properties of seismicity? In: R. Cassinini and G.F. Panza (Editors), *The Structure of the Alpine-Mediterranean area: Contribution of Geophysical Methods*. *Terra Nova*, 2: 585-595.

Patacca, E., Sartori, R. and Scandone, P., 1992. Tyrrhenian basin and Apenninic arcs: kinematic relations since late Tortonian times. *Mem. Soc. Geol. Ital.*, in press.

PFG, 1985. Catalogo dei terremoti italiani dall'anno 1000 al 1980 [Edited by D. Postpischl]. CNR, Prog. Final. Geodin., Roma, pp. 1-239.

Scarascia, S. and Pellis, G., 1985. Crustal structure of the Northern Apennine. Part A—The upper crust. In: D.A. Galson and St. Mueller (Editors), *Proc. 2nd Workshop on the European Geotraverse (EGT) Project, The Southern Segment*. European Science Fundation, Strasbourg, pp. 137-142.

Schütte, K.G., 1978. Crustal structure of Southern Italy. In: H. Closs, D. Roeder and K. Schmidt (Editors), Alps, Apennines and Hellenides. IUGG, 38: 374–388.

Suhadolc, P., 1990. Fault-plane solutions and seismicity around the EGT southern segment. In: R. Freeman and St. Mueller (Editors), Proc. 6th Workshop on the European Geotraverse (EGT), Data compilations and synoptic interpretation. European Science Foundation, Strasbourg, pp. 371–382.

Suhadolc, P., Panza, G.F., Marson, I., Costa, G. and Vaccari, F., 1992. Analisi della sismicità e meccanismi focali nell'area italiana. Atti Conv. Gruppo Naz. Difesa Terremoti, Pisa, 1990, 1: 157–168.

Vaccari, F., Suhadolc, P. and Panza, G.F., 1990. Irpinia, Italy, 1980 earthquake: waveform modelling of strong motion data. *Geophys. J. Int.*, 101: 631–647.

Woppard, G.P., 1975. Regional changes in gravity and their relation to crustal parameters. *Bur. Grav. Int. Bull. Inf.*, 36: 106–110.

